UCRL-ID-154021

Microstructure and Fracture Behavior of Tungsten Heavy Alloys

A. Sunwoo

June 2003

U.S. Department of Energy

Lawrence
Livermore
National
Laboratory

Work performed under the auspices of the U. S. Department of Energy by the University of California Lawrence Livermore National Laboratory under Contract W-7405-Eng-48.

Microstructure and Fracture Behavior of Tungsten Heavy Alloys

Anne Sunwoo

Lawrence Livermore National Laboratory

Summary

The 93% W-5.6% Ni-1.4% Fe and 93.1% W-4.7% Ni-2.2% Co alloys (WHA) provided by Army Research Laboratory (ARL), Aberdeen are characterized to determine the effects of matrix alloying and swaging on the microstructure and fracture behavior. The W particles are oblong with respect to the swaging direction. The microstructure of the W-Ni-Fe alloy reveals good cohesive bonding between W particles, but there is W-matrix interface separation and matrix alloy cracking. The microstructure of the W-Ni-Co alloy reveals regions of good cohesive bonding between W particles, but also regions where some wetting has not occurred by the liquid. No evidence was observed of matrix alloy cracking. The fracture characteristic of WHA is dominantly cleavage of W particles.

Background

Tungsten heavy alloys are typically produced using the liquid phase sintering (LPS) method. The matrix alloy systems are either Ni-Fe or Ni-Co. In the W-Ni-Fe system, Ni wets W powder surfaces to form a NiW_2 intermetallic compound [Brandes]. The Fe is added to react with Ni to form a eutectic at 1440°C [ASM handbook]. To produce uniform hardness through the diameter of the rod, and as a way of strengthening, the rods are commonly cold swaged.

For the W-Ni-Co system, Co also forms an intermetallic compound, Co_7W_6 [Brandes]. Depending on the LPS temperature, both Ni and Co will compete to form the W-X intermetallic compound.

Two WHA fractured specimens were provided by ARL to characterize the microstructure and fracture characteristics [Bjerke]. A flat specimen of the 93% W-5.6% Ni-1.4% Fe alloy is from the fracture test. The parent material is a bar that was swaged to 20%

reduction in diameter and aged. The flat specimen was made in the long-transverse direction and the W particles are elongated along the direction of the bar axis. A round penetrator bar specimen of the 93.1% W-4.7% Ni-2.2% Co alloy is from a terminal ballistic experiment. Both specimens were broken transverse to the swaging direction. The basic properties of the alloys are given in Tables 1 and 2. Although the composition is different, the densities are comparable. The particle sizes had an effect on the yield strength, via the Hall-Petch relation, and with high strength, ductility is sacrificed.

Three possible fracture phenomena are expected in the WHA: cleavage of the W particles, separation at W-W interfaces and fracture of the matrix. Given the brittleness of W, the dominant fracture mechanism should be cleavage of the W particles.

Characterization

Microstructure

Figure 1a shows the microstructure of the W-Ni-Fe alloy. The W particles are slightly oblong in the swaging direction. Closer examination of the W particles suggests some particles are in intimate contact, such that the boundaries are not discernible. The average W particle size was about 35-38 μm. The SEM micrograph of the polished specimens in Figure 1b reveals cohesive bonding of W particles, separation between W and matrix, and cracking of Fe-Ni matrix. The Fe-Ni system undergoes several phase transformation from liquid to solid. Shrinkage and phase transformation of the matrix alloy and swaging effects during processing could have contributed to the W-matrix interface separation and matrix cracking.

The W particles found in the W-Ni-Co alloy in Figure 2a are smaller and less elongated than those in the W-Ni-Fe alloy, which could be due to the amount of swaging the rod received. However, microvoids on W particles are equally present in both alloys. There are some impurities present in the rod showing up as dark rings. In Figure 2b, SEM micrograph of the polished surface reveals no separation between W and matrix, or matrix cracking. The microstructure has regions in which there appears to be no wetting of the W particles by the Ni-Co liquid phase, or ruffled and semi-dendritic protrusions, indicative of intermetallic compound formation, (Figure 2b). Unlike the Ni-Fe system, Ni and Co are completely soluble with each other. The finer particles in the W-Ni-Co alloy exhibited higher hardness and yield strength.

Fractography

Fractography of the W-Ni-Fe specimen is shown in Figure 3. This figure clearly illustrates the cleaved W particles, as well as evidence of separation between neighboring W particles. A crack nucleation point can be readily observed on individual W particles, based on the appearance of fan-like striations on the fracture surface. The appearance of these fan-like striations, of varying orientation, may suggest multiple crack nucleation sites or crack branching or changes in the crack path. Figure 3 also indicates the presence of transverse cracks, i.e., cracks that appear to be normal to the primary fracture surface. These transverse cracks may have formed during swaging process and opened up under tensile loading. In other words, initial deformation and incipient crack formation of the W-particles were already present in the alloy. Fracturing along the long-transverse direction resulted in the creation of the fan-like striations. The striations of the transverse cracks give the appearance of having once been continuous (see Figure 3b).

The W-Ni-Co alloy bar specimen was made parallel to the swaging direction and impact tested at 1300 m/s velocity [Bjerke]. Figure 4 displays the fracture surfaces of the alloy. Qualitatively, the fracture surface appears less tortuous than that of the W-Ni-Fe alloy; suggesting the W-Ni-Co alloy is less ductile. The fracture is predominantly due to cleavage of the W particles, with less evidence of W-W particle separation, indicating a robust W-X intermetallic compound bond between W and Ni-Co- matrix. Whereas the fracture surface of the W particles is generally similar to those observed in the W-Ni-Fe alloy, some differences exist in surface topography. In both the W-Ni-Fe and W-Ni-Co alloys, fracture of the W particles gives rise to the fan-like striations. However, in the latter alloy additional features that are absent in the W-Ni-Fe alloy accompany these striations. These features appear as layering or ledges superimposed on the striations, cf. Figures 4b-4d. Similarly to the W-Ni-Fe alloy, transverse cracking is also apparent. In addition to the swaging effect, the terminal ballistic impact may induce compressive loading in the alloy, followed by tensile loading, leading to ultimate tensile fracture.

Recommendations

For WHA that fractures under a dynamic tensile loading condition the desired material properties are high dynamic tensile strength and high dynamic fracture toughness.

To obtain this inverse relationship in the material properties, the particle size refinement on isotropic dynamic fracture toughness and tensile properties is proposed. The characterization of the WHA indicates that the W particle size is about 35 μm and the dominant fracture mode is the cleavage of W particles. A finer W particle size would enhance both tensile yield strength and fracture toughness of the alloy. The reduction in W particle size would have a less effect on the compressive strength [Ramesh and Coates].

Swaging/cold working strain hardens the ductile matrix but can cause internal damage to W particles. Working W particles with a limited deformability under tensile forces ultimately leads to cracking. When tested along the metal flow direction, the dynamic fracture toughness values were lower than the orthogonal direction [Rittel and Weisbrod]. Aging the swaged WHA rod may strengthen the ductile matrix, but it will not mitigate the damage to the W particles. As seen in the micrographs, about 20μm W particles maintain their shape.

Acknowledgments

The author would like to thank Dr. Dana Goto for his critical review and inputs. This work was performed under the auspices of the U. S. Department of Energy by the Lawrence Livermore National Laboratory under Contract No. W-7405-Eng-48.

References

E. A. Brandes, Smithells Metals Reference Book, 6th ed. Butterworths, London, 1983.

ASM Handbook, Alloy Phase Diagrams, vol.3, ASM Intl, Materials Park, 1992.

T. W. Bjerke, "KE Penetrator Fracture Program," WHPR01D, WHPR Work Area Review, December 2002.

K. T. Ramesh and R. S. Coates, "Microstructural Influences on the Dynamic Response of W HA," Metal. Trans. A, 23A, 2625, 1992.

D. Rittel and G. Weisbrod, " Dynamic fracture of W base heavy alloys," Intl J Fracture, 212, 87, 2001.

Table 1. Properties of WHA [Bjerke '02].

Samples	UTS (GPa)	YS (GPa)	Elong. (%)	Density (g/cc)	Hardness (HR_c)
W-5.6Ni-1.4Fe[1]	1.425	1.19	12.5	17.8	-
W-4.7Ni-2.2Co[2]	1.420	1.39	8.9	17.7	43.2

[1] Data determined by Osram Sylvania. A bar was swaged to 20% reduction in area and aged.

[2] Sample ID# 's ARL 7/9-1 to -3 were tested at Aerojet Ordnance Tennessee.

Table 2. Measured particle size and hardness values of WHA.

Samples (wt-%)	Particle size (μm)	Vickers (VHN) Kg/mm^2	Hardness (HR_c)[1]
W-5.6Ni-1.4Fe	35-38	451	45
W-4.7Ni-2.2Co	30-35	492	48

[1] Converted from Vickers hardness numbers (VHN).

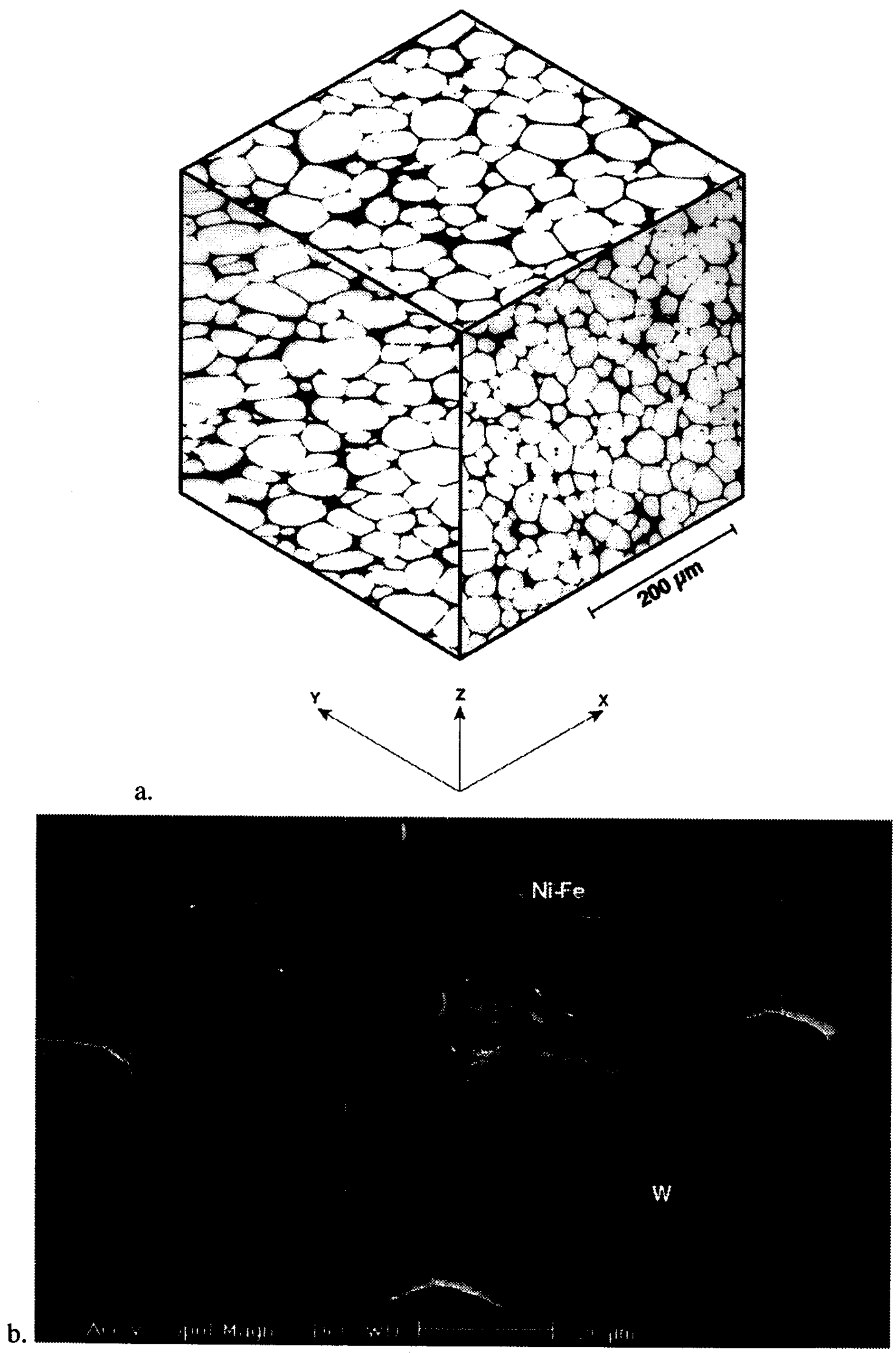

Figure 1. a) 3-D optical micrograph of the W-Ni-Fe alloy and b) SEM micrograph showing cohesive bonding of W, debonding at the interface, and cracking of the matrix.

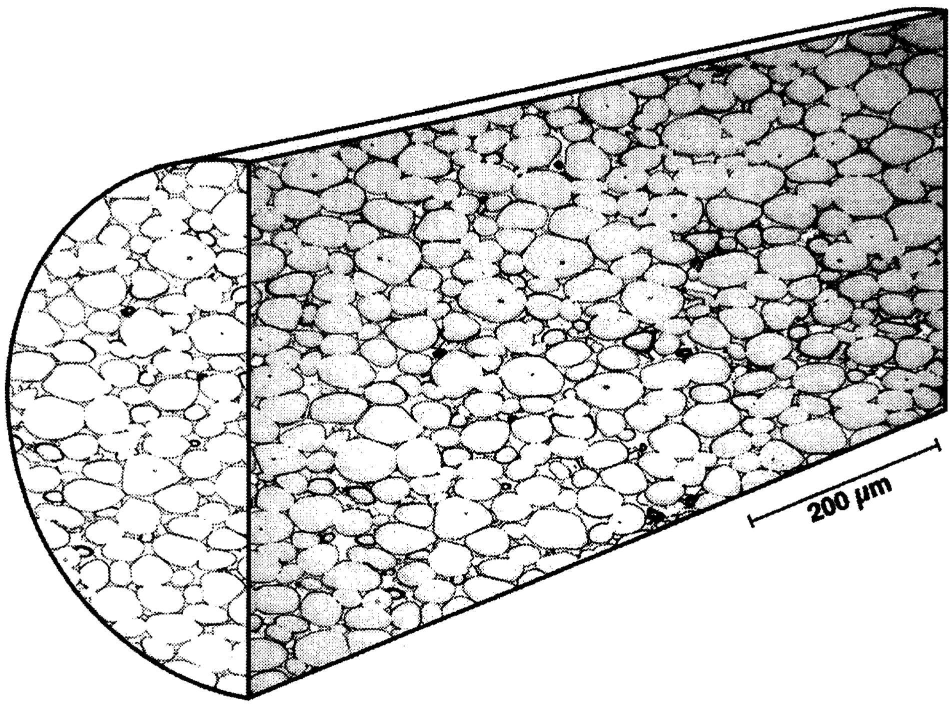

a.

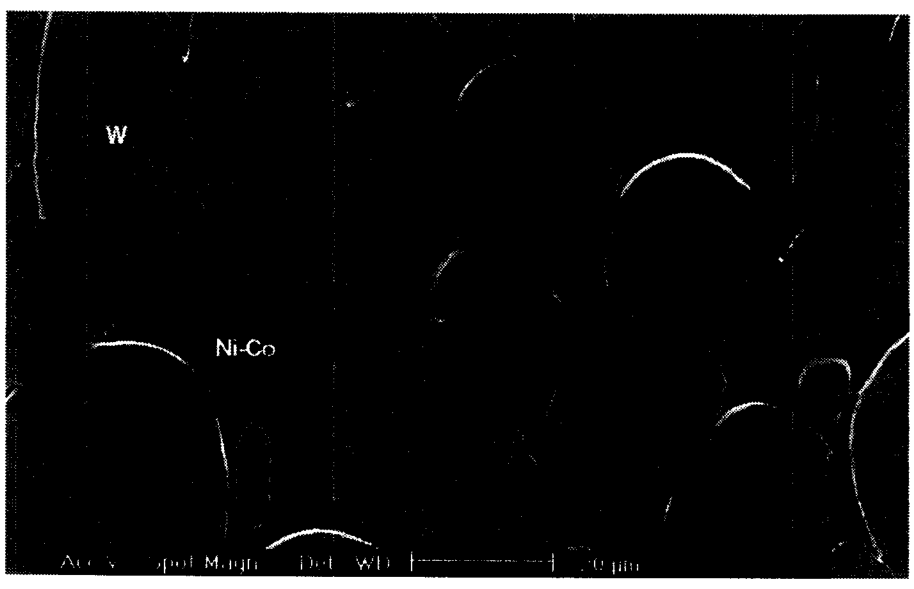

b.

Figure 2. a) 2-D optical micrograph of the W-Ni-Co alloy rod and b) SEM micrograph showing cohesive bonding of W, and complete and incomplete wetting at the interface.

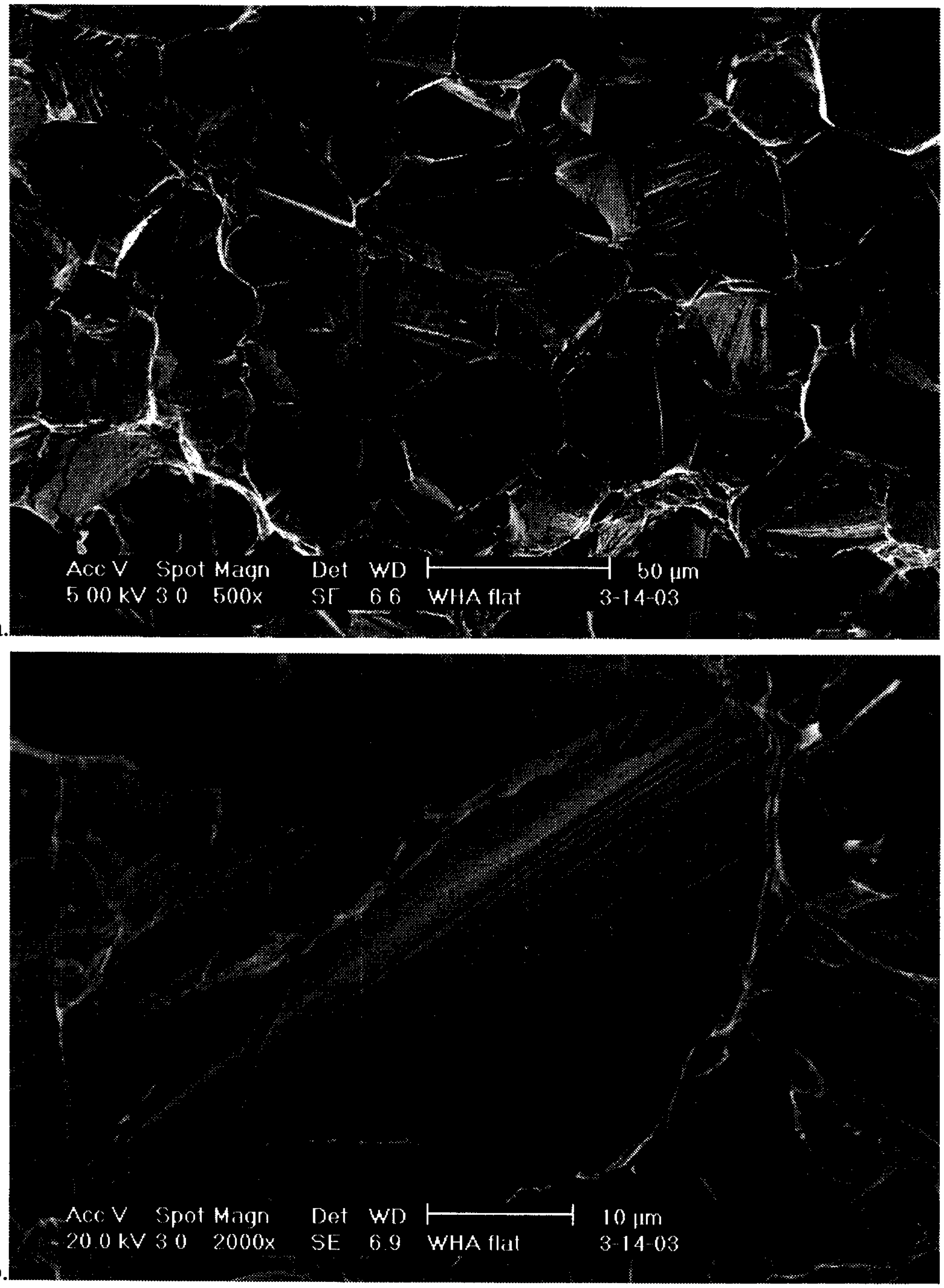

a.
b.
Figure 3. Fracture surfaces of W-Ni-Fe alloy.

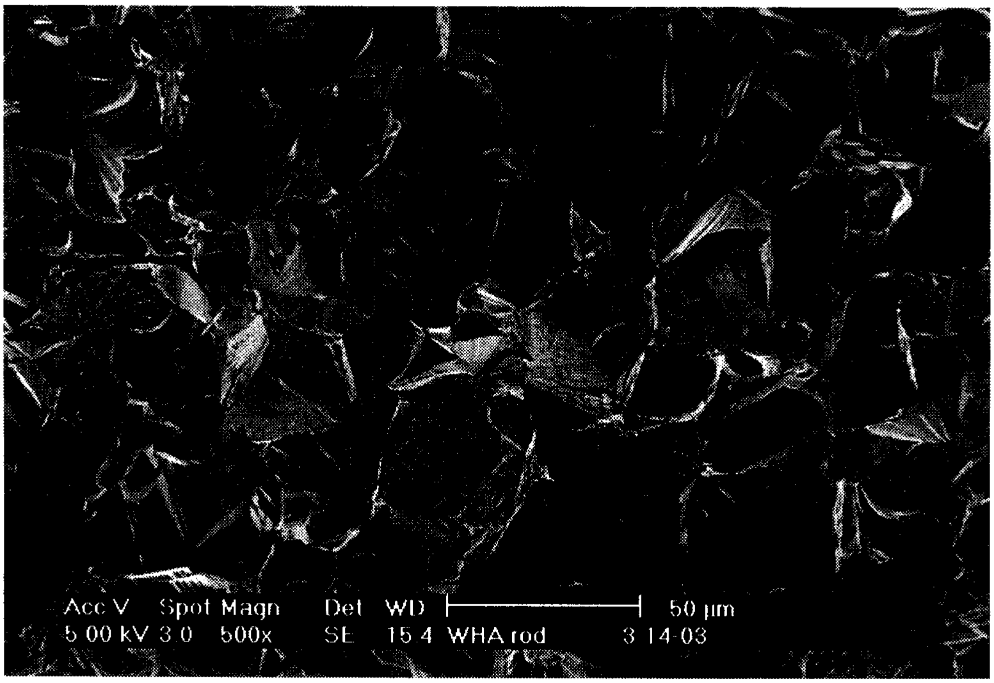
Acc V Spot Magn Det WD 50 µm
5 00 kV 3 0 500x SE 15 4 WHA rod 3 14 03
a.

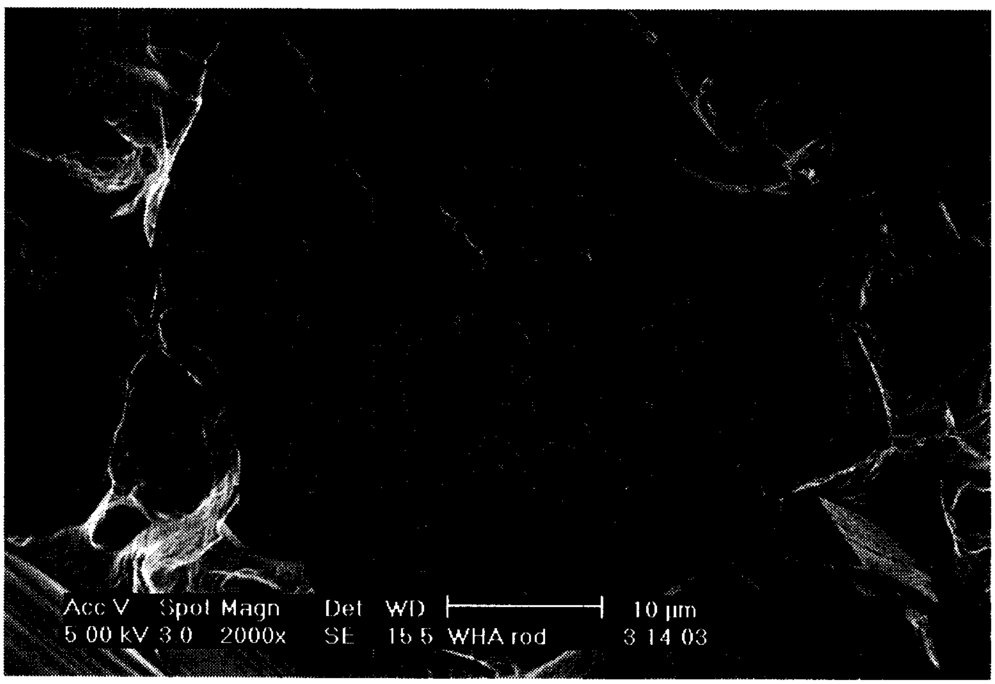
Acc V Spot Magn Det WD 10 µm
5 00 kV 3 0 2000x SE 15 5 WHA rod 3 14 03
b.

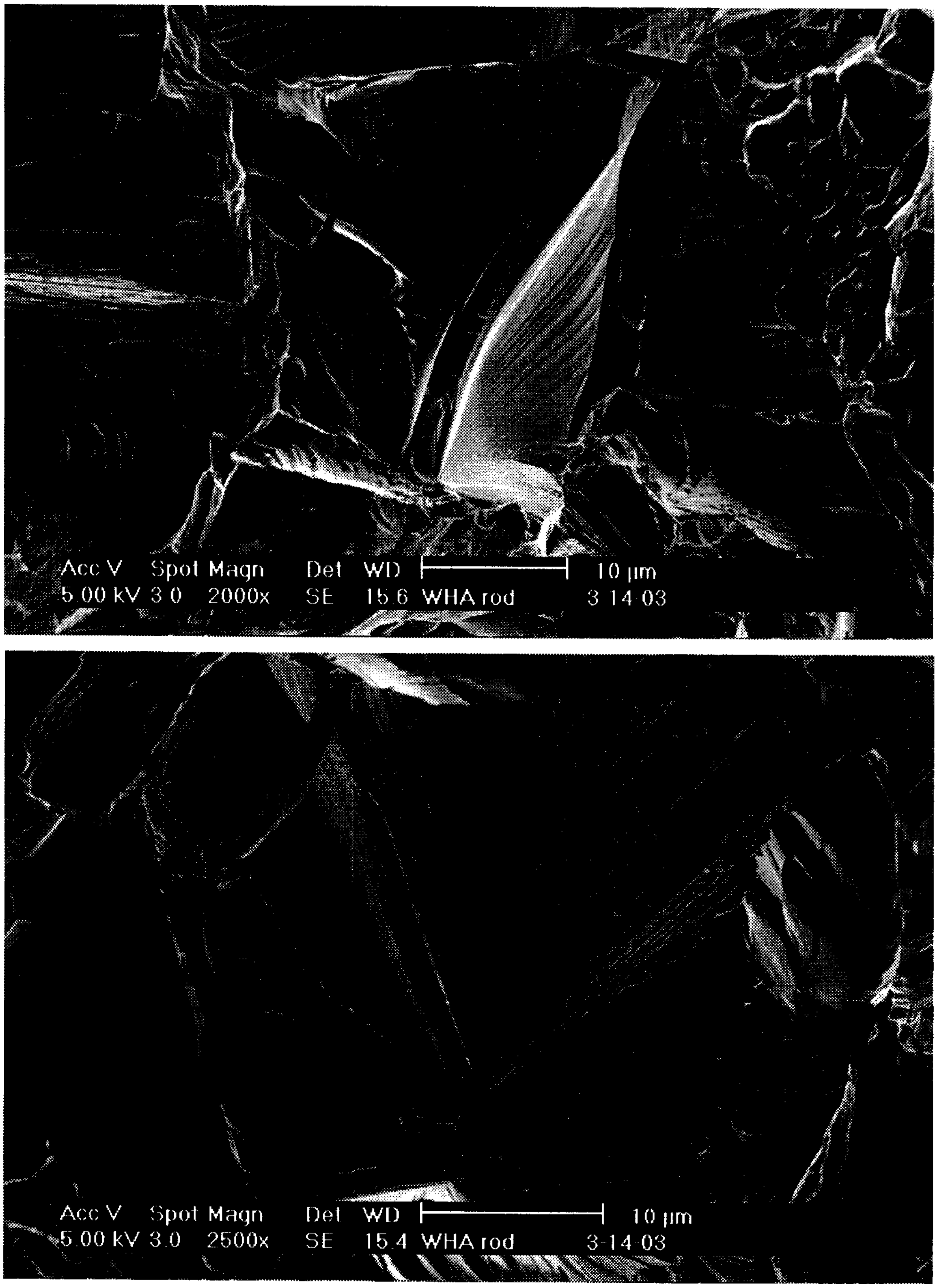

c.

d.

Figure 4. Fracture surfaces of W-Ni-Co alloy.

University of California
Lawrence Livermore National Laboratory
Technical Information Department
Livermore, CA 94551